



Structural and functional studies with mytoxin II from *Bothrops moojeni* reveal remarkable similarities and differences compared to other catalytically inactive phospholipases A₂-like

Guilherme H.M. Salvador^{a,1}, Walter L.G. Cavalcante^{a,b,1}, Juliana I. dos Santos^{a,1}, Márcia Gallacci^b, Andreimar M. Soares^c, Marcos R.M. Fontes^{a,*}

^a Depto. de Física e Biofísica, Instituto de Biociências, UNESP – Univ Estadual Paulista, Botucatu, SP, Brazil

^b Depto. de Farmacologia, Instituto de Biociências, UNESP – Univ Estadual Paulista, Botucatu, SP, Brazil

^c Centro de Estudos de Biomoléculas Aplicadas à Saúde, CEBio, Fundação Oswaldo Cruz, FIOCRUZ Rondônia e Departamento de Medicina, Universidade Federal de Rondônia, UNIR, Porto Velho, RO, Brazil

ARTICLE INFO

Article history:

Received 15 February 2013

Received in revised form 16 May 2013

Accepted 11 June 2013

Available online 25 June 2013

Keywords:

Lys49-phospholipase A₂
Bothrops moojeni venom
 Oligomeric assembly
 X-ray crystallography
 Myographic studies

ABSTRACT

Lys49-phospholipases A₂ (Lys49-PLA₂s) are proteins found in bothropic snake venoms (Viperidae family) and belong to a class of proteins which presents a phospholipase A₂ scaffold but are catalytically inactive. These proteins (also known as PLA₂s-like toxins) exert a pronounced local myotoxic effect and are not neutralized by antivenom, being their study relevant in terms of medical and scientific interest. Despite of the several studies reported in the literature for this class of proteins only a partial consensus has been achieved concerning their functional–structural relationships. In this work, we present a comprehensive structural and functional study with the MjTX-II, a dimeric Lys49-PLA₂ from *Bothrops moojeni* venom which includes: (i) high-resolution crystal structure; (ii) dynamic light scattering and bioinformatics studies in order to confirm its biological assembly; (iii) myographic and electrophysiological studies and, (iv) comparative studies with other Lys49-PLA₂s. These comparative analyses let us to get important insights into the role of Lys122 amino acid, previously indicated as responsible for Lys49-PLA₂s catalytic inactivity and added important elements to establish the correct biological assembly for this class of proteins. Furthermore, we show two unique sequential features of MjTX-II (an amino acid insertion and a mutation) in comparison to all bothropic Lys49-PLA₂s that lead to a distinct way of ligand binding at the toxin's hydrophobic channel and also, allowed the presence of an additional ligand molecule in this region. These facts suggest a possible particular mode of binding for long-chain ligands that interacts with MjTX-II hydrophobic channel, a feature that may directly affect the design of structure-based ligands for Lys49-PLA₂s.

© 2013 Elsevier Ltd. All rights reserved.

1. Introduction

Envenoming by snakebites represents a relevant and neglected global health problem, particularly in tropical

regions (Gutierrez et al., 2006; Harrison et al., 2009; Russell, 1991). Recent estimates indicate that at least 421,000 envenomations and 20,000 deaths related to ophidian accidents occur each year, mainly in Latin America, Asia and Africa (Kasturiratne et al., 2008); however, this same study suggests that these numbers can be as high as 1,841,000 envenomations and 94,000 deaths (Kasturiratne et al., 2008). Even so, the mortality caused by snakebite is

* Corresponding author. Tel.: +55 14 38800271; fax: +55 14 38153744.

E-mail address: fontes@ibb.unesp.br (M.R.M. Fontes).

¹ These authors contributed equally to this work.

much higher than the given by several neglected tropical diseases, such as dengue haemorrhagic fever, leishmaniasis, cholera, schistosomiasis and Chagas disease, which leads the World Health Organization to include the ophidian accidents in the list of neglected tropical diseases (Williams et al., 2010).

Snakes from Viperidae family are found in many parts of the world causing several accidents every year (Gutierrez and Lomonte, 1995; Kasturiratne et al., 2008). Particularly in Brazil, the majority of ophidian accidents occur with the *Bothrops* genus (Viperidae family) (Rosenfeld and Kelen, 1971; Saúde, 2001) that are characterized by pronounced local effects, including hemorrhage, edema, pain and myonecrosis (Gutierrez and Chaves, 1980; Gutierrez and Ownby, 2003; Homs-Brandeburgo et al., 1988; Mebs et al., 1983; Queiroz and Petta, 1984; Rosenfeld and Kelen, 1971). These local effects are very relevant in terms of medical and scientific interest since the proteins responsible for the toxic process which may lead to permanent tissue loss, disability and, in some cases may require the amputation of the victim's affected limb are not efficiently neutralized by antivenom administration (Gutierrez and Lomonte, 1995).

Phospholipases A₂ (PLA₂s) are enzymes that catalyze the hydrolysis of glycerophospholipids, in a calcium-dependent manner, and represent the most abundant myotoxic components in Viperidae snake venoms (Gutierrez and Ownby, 2003). These proteins can be classified into two groups according to their evolutionary pathway: i) the catalytically active enzymes, such as Asp49-, Asn49- and Gln49-PLA₂s and ii) the catalytically inactive PLA₂ variants (Lys49-, Arg49-, and some Asp49-PLA₂s) (dos Santos et al., 2011b). In this latter group, the most studied toxins are the basic and homodimeric Lys49-PLA₂s that induce noticeable local myonecrosis by means of a calcium-independent mechanism (Lomonte and Rangel, 2012). In addition, Lys49-PLA₂s exhibit some effects found exclusively *in vitro*, as the blockade of neuromuscular transmission in isolated preparations, which has been directly associated to their ability in destabilizing cell membranes (Gallacci and Cavalcante, 2010; Correia-de-Sa et al., 2013). Although these toxins are not able to block neuromuscular transmission *in vivo*, it may be a useful experimental approach to investigate both the mechanism of action and the structural–activity relationship of the myotoxic Lys49-PLA₂s.

In this work we report structural and functional studies with a basic Lys49-PLA₂ from *Bothrops moojeni*, known as Myotoxin II or MjTX-II. *B. moojeni* snakes are found in central and southeastern part of the Brazil and also in some parts of Argentina, Paraguay and Bolivia, living mainly in “cerrado” and “araucaria forests” ecosystems (Borges and Araujo, 1998). Their study have clinical and scientific importance because of the number of accidents caused by these snakes due to their aggressive behavior, their large size compared to other snakes from the same genus and because their adaptive capacity against environmental changes (Melgarejo, 2003). MjTX-II has 122 amino acids, molecular weight of approximately 13.5 kDa (Lomonte et al., 1990; Watanabe et al., 2005), and presents myotoxic activity that is characterized by increase of serum

creatine kinase and morphologic changes in mice muscles when studied *in vivo* and *in vitro* (Stabeli et al., 2006; Cavalcante et al., 2007). In addition, it was demonstrated that this protein presents antimicrobial, antitumoral and antiparasitic effects, having therefore potential to therapeutic applications (Stabeli et al., 2006).

Although the crystal structure of MjTX-II had been reported in the literature in 1997 (de Azevedo et al., 1997), the article just presents the comparison of this structure with BaspTX-II (myotoxin II from *Bothrops asper*) that was the only Lys49-PLA₂ structure known at that data. Furthermore, the authors did not deposit the coordinates of MjTX-II structure in PDB data bank making any comparison with other structures impossible. In 2005, the structure of the complex formed between MjTX-II and stearic acid was solved (Watanabe et al., 2005), revealing the ligand binding sites and comparing it to PrTX-II/fatty acid structure that was solved in 2001 (Lee et al., 2001). Since then, several structures of native and complexed Lys49-PLA₂s have been solved revealing some consensual features of these proteins (e.g. homodimeric conformation) but bringing many controversial and intriguing issues (e.g. biological assembly, myotoxic site, the role of Lys122 residue) (Murakami et al., 2005; dos Santos et al., 2009; Fernandes et al., 2010; Marchi-Salvador et al., 2009; dos Santos et al., 2011b). Then, in this article we try to definitively address these issues for Lys49-PLA₂s in general and to highlight some specific characteristics of MjTX-II which may be very important considering the medical and scientific importance of Lys49-PLA₂s proteins for the establishment of myonecrosis.

2. Materials and methods

2.1. Crystallization, X-ray data collection and data processing

A lyophilized sample of MjTX-II was dissolved in ultrapure water at a concentration of 11 mg mL⁻¹. MjTX-II crystals were obtained by the hanging-drop vapor-diffusion method (Ducruix and Giegé, 1992) in which 1 μl protein solution and 1 μl reservoir solution were mixed and equilibrated against 500 μl of the precipitant solution. Single crystals were obtained using a solution containing 20% (v/v) 2-propanol, 20% (w/v) polyethylene Glycol 4000 and 1.0 M Sodium Citrate pH 5.6. The crystals measured 0.30 × 0.25 × 0.15 mm after growing approximately one month at 291 K.

X-ray diffraction data were collected using wavelength of 1.423 Å at a synchrotron-radiation source (MX2 beamline – Laboratório Nacional de Luz Síncrotron, LNLS, Campinas, Brazil) using a MAR CCD imaging-plate detector (MAR Research™). The crystals submitted to X-ray diffraction experiments were held in appropriate nylon loops and flash-cooled in a stream of nitrogen at 100 K without cryoprotectant. The best data set was collected with a crystal-to-detector distance of 75 mm and an oscillation range of 1° resulting in 104 images collected. The data were processed at 1.92 Å resolution using the HKL program package (Otwinowski and Minor, 1997) showing the crystals belong to P2₁2₁2₁ space group and that they are isomorphous to the crystals of MjTX-II complexed to stearic

acid (Watanabe et al., 2005). X-ray diffraction data processing and refinement statistics are shown in Table 1.

2.2. Structure determination and refinement

The crystal structure was solved by the Molecular Replacement Method using the program MOLREP (Vagin and Teplyakov, 1997) from CCP4 package v.6.1.13 (Potterton et al., 2004) and atomic coordinates of MjTX-II/stearic acid complex (monomer A with the stearic acid ligand omitted was used - PDB access code 1XXS) (Watanabe et al., 2005). Rounds of crystallographic refinement with CNS v.1.3 (Brunger et al., 1998) and manual modeling using the program Coot v.0.7 (Emsley and Cowtan, 2004) were used to improve the model, considering R_{cryst} and free R-factors. Polyethylene glycol (PEG) 4000, isopropanol and solvent molecules were added by CNS v.1.3 and Coot v.0.7 programs. Due to the lack of electron density in some regions of the model, the following amino acid side chains were not modeled: monomer A - Lys16, Lys 36, Lys70, Glu86, Asn88 and Lys128; monomer B - Lys16, Lys57, Lys69, Lys70 and Lys128. The final model was checked in MolProbity program (<http://molprobity.biochem.duke.edu/>) (Chen et al., 2010). The coordinates were deposited in the Protein Data Bank with identification code 4KF3.

2.3. Comparative analysis

Molecular comparisons of the structures were performed using the Coot v.0.7 program (Emsley and Cowtan, 2004) with only C_{α} coordinates. The structures of MjTX-II/stearic acid (PDB ID 1XXS) (Watanabe et al., 2005), BaspTX-II (PDB ID 1CLP) in its native form (Arni et al., 1995)

and complexed to suramin (PDB ID 1Y4L) (Murakami et al., 2005), BthTX-I (PDB ID 3HZD), BthTX-I/PEG4000 (PDB ID 3IQ3), BthTX-I/BPB (PDB ID 3HZW), PrTX-I/BPB (PDB ID 2OK9) (Fernandes et al., 2010), BthTX-I/ α - tocopherol (PDB ID 3CXI), PrTX-I (PDB ID 2Q2J), PrTX-I/ α - tocopherol (PDB ID 3CYL) (dos Santos et al., 2009), PrTX-I/Rosmarinic acid (PDB ID 3QNL) (dos Santos et al., 2011a), PrTX-II/fatty acid (PDB ID 1QLL) (Lee et al., 2001), BnSP-6 and BnSP-7 (PDB ID 1PC9 and 1PA0 respectively) (Magro et al., 2003) and BnIV/Myristic acid (PDB ID 3MLM) (Delatorre et al., 2011) were used in the comparative analysis.

All the structural figures were generated using the Pymol program (DeLano, 2002). Analysis of the quaternary assemblies and interfacial contacts of the crystallographic models were performed using the online interactive tool PISA (Krissinel and Henrick, 2007) available at the European Bioinformatics Institute server (<http://www.ebi.ac.uk>).

2.4. Dynamic light scattering

Dynamic light scattering (DLS) experiments were executed at 283 K using a DynaPro TITAN™ (Wyatt Technology™) device. One hundred measurements were acquired with the protein dissolved in ultra-pure water at 3.5 mg mL⁻¹ concentration. Analyses of these data were performed with Dynamics v.6.10 program (Wyatt Technology™).

2.5. Myographic study

Adult male Swiss mice (20–25 g) were killed by exsanguination after cervical dislocation. The mouse phrenic nerve-diaphragm muscle was removed and mounted vertically under a tension of 5 g in a conventional isolated organ bath chamber containing 15 ml of Ringer solution, with the following composition (mol/l): NaCl, 135; KCl, 5; MgCl₂, 1; CaCl₂, 2; NaHCO₃, 15; Na₂HPO₄, 1; glucose, 11. This solution was gassed with O₂ (95%) + CO₂ (5%) and kept at 35 ± 2 °C. The preparation was attached to an isometric force transducer (Grass, FT03) coupled to a signal amplifier (Gould Systems, 13-6615-50). The recordings were made on a computer through data acquisition system (Gould Sytems, Summit ACQUIRE and Summit DataViewer). The preparation was stabilized for at least 45 min before the toxin addition. Indirect contractions were evoked by supramaximal strength pulses (0.2 Hz; 0.5 ms; 3 V), delivered by an electronic stimulator (Grass S88K) and applied on the phrenic nerve by suction electrode. Direct contractions were evoked by supramaximal pulses (0.2 Hz; 5 ms; 13 V) through a bipolar electrode positioned on opposite sides of the muscle. Experiments of direct contractions were performed in the presence of D-tubocurarine (5 µg/ml) previously to toxin addition. The amplitudes of indirect and direct twitches were evaluated during 90 and 120 min respectively and the time required to reach 50% paralysis ($t_{1/2}$) was determined in each situation.

2.6. Electrophysiological study

The mouse phrenic diaphragm muscle was removed and fixed in an isolated organ bath chamber containing 5 ml of Ringer solution. The resting membrane potentials

Table 1

X-ray data collection and refinement statistics for the MjTX-II crystallographic structure.

Unit cell (Å)	$a = 50.0; b = 62.2; c = 86.0$
Space group	P2 ₁ 2 ₁ 2 ₁
Resolution (Å)	50.00–1.92 (1.99–1.92) ^a
Unique reflections	19571 (2036) ^a
Completeness (%)	92.4 (97.6) ^a
$I/\sigma(I)$	10.4 (2.0) ^a
Redundancy	3.9 (3.7) ^a
Molecules in ASU	2
Matthews coefficient V_M (Å ³ Da ⁻¹)	2.5
R_{merge}^b (%)	11.0 (41.9) ^a
R_{cryst}	22.8
R_{free}	25.7
Number of non-hydrogen atoms	
Protein	1916
Waters	186
PEG molecules	4
Isopropanol molecules	6
Mean B-factor (Å ²) ^c	
Overall	56.12
Ramachandran plot (%) ^d	
Residues were in favored	96.7
Residues were in allowed	3.3

^a Numbers in parenthesis are for the highest resolution shell.

^b $R_{\text{merge}} = \sum_{hkl} [\sum_i (I_{hkl,i} - \langle I_{hkl} \rangle)] / \sum_{hkl} \langle I_{hkl} \rangle$, where $I_{hkl,i}$ is the intensity of an individual measurement of the reflection with Miller indices h, k and l , and $\langle I_{hkl} \rangle$ is the mean intensity of that reflection. Calculated for $I > -3\sigma(I)$.

^c Calculated with CNS program.

^d Calculated with MolProbity program.

(MP) and miniature endplate potentials (MEPP) were measured by standard microelectrode techniques (Fatt and Katz, 1951). The glass microelectrodes were filled with 3 M KCl and introduced intracellularly in the muscle fibers with a micromanipulator (Leitz). Microelectrodes were attached to a preamplifier (World Precision Instruments, Electro 70s) coupled to an amplification system (Biopac Systems, MP450) and monitored on an oscilloscope (Tektronix, 2232) and on a computer with a data acquisition and analysis system (AcqKnowledge®, version 3.8.2). The resting MP was recorded at times 5, 15, 30, 60 and 90 min and MEPPs at 5, 30, 60 and 90 min after MjTX-II administration. Recording sites were rejected if the membrane potential was less than -65 mV on the initial impalement.

2.7. Ethics

Institutional Animal Care and Use Committee (Institute of Biosciences – Sao Paulo State University – UNESP) approved this study under the number 033/05. Animal procedures were in accordance with the guidelines for animal care prepared by the Committee on Care and Use of Laboratory Animal Resources, National Research Council, USA.

2.8. Statistical analysis

Results are expressed as mean \pm S.E. Data were analyzed by ANOVA complemented by the Tukey–Kramer test. Values of $P < 0.05$ were considered significant.

3. Results and discussion

3.1. Overall crystallographic structure

The crystal structure of MjTX-II was solved at 1.92 Å resolution revealing an asymmetric unit containing two monomers. As shown in Table 1, the refinement of the model converged to a final R_{cryst} of 22.8% and an R_{free} of 25.7%. The final model is constituted by 1916 non-hydrogen protein atoms, 186 water, four polyethylene glycol 4000 (PEG4K) and six isopropanol molecules. The overall stereochemical quality of the final MjTX-II structure was judged as satisfactory since 96.7% and 100% of the total number of amino acid residues are located in the favored and allowed regions of the Ramachandran plot respectively, according to their ϕ/ψ angle combinations. MjTX-II structure is stabilized by seven disulfide bridges and preserves the classical secondary structure elements found in this group of proteins, i.e., an N-terminal α -helix, a “short” helix, a non-functional Ca^{2+} -binding loop, two anti-parallel α -helices (2 and 3), two short strands of anti-parallel β -sheet (known as β -wing), and a C-terminal loop (Fig. 1A). MjTX-II structure presents four PEG4K molecules interacting with it (Fig. 2): (i) two PEG4K (PEG 1 and 2) molecules are found inside of the hydrophobic channels (one molecule in each protein protomer), displaying hydrogen bond with Gly30 and also other interactions with “active site” residues; (ii) one PEG4K (PEG 3) molecule interacts at the same time with the residues Lys49 and Tyr52 from both

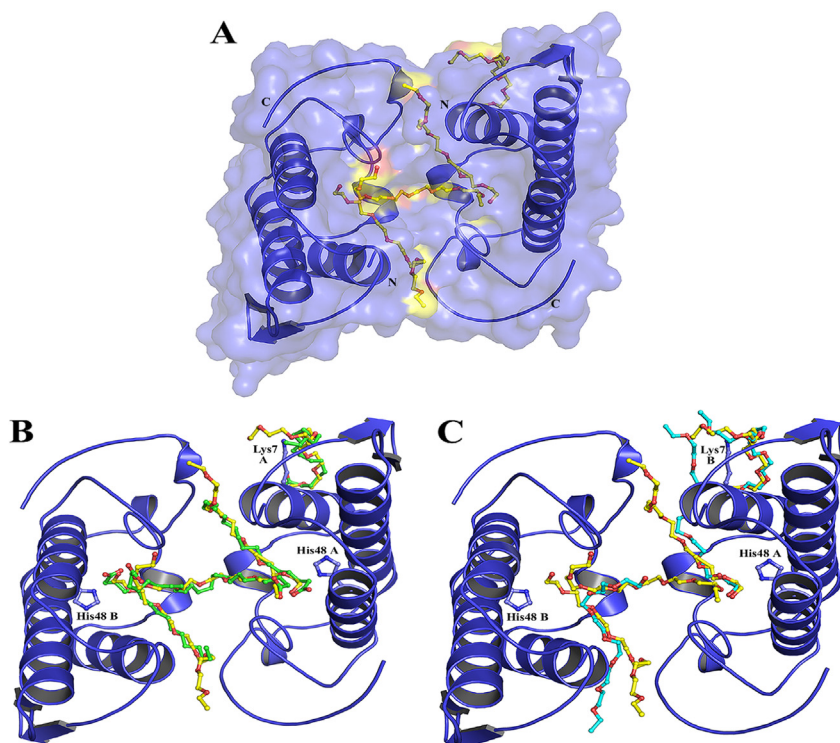


Fig. 1. Crystal structure of MjTX-II (A) and its superposition with MjTX-II/stearic acid (B) and with BthTX-I/PEG4K (C). The protein is represented in cartoon and ligand molecules are shown in sticks: in yellow, PEG4K from MjTX-II structure, in green, stearic acid molecules from MjTX-II/stearic acid structure and in cyan, PEG4K from BthTX-I/PEG4K structure. Drawn using PyMol program (DeLano, 2002). (For interpretation of the references to colour in this figure legend, the reader is referred to the web version of this article.)

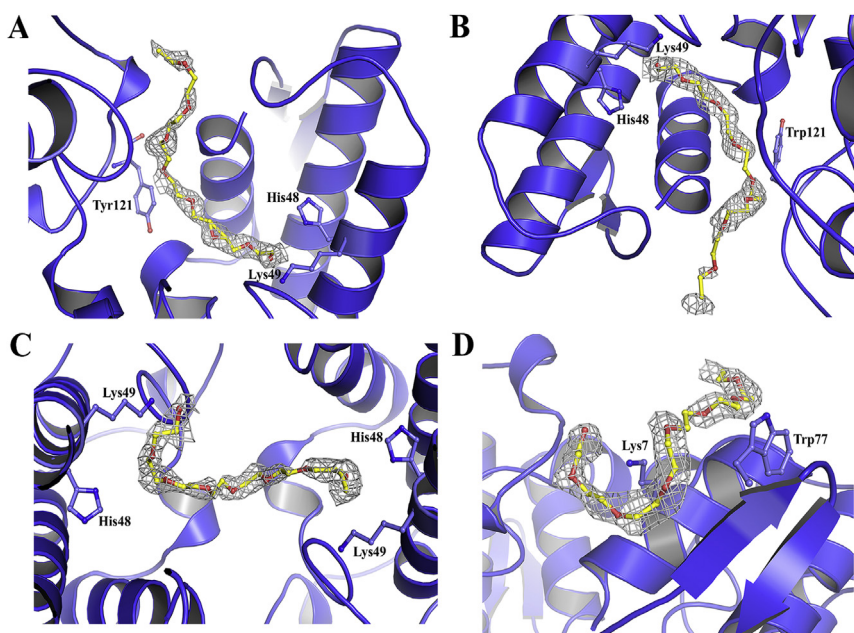


Fig. 2. Electron density difference maps for PEG4K molecules from the MjTX-II structure: (A) PEG4K (1) in the hydrophobic channel region of monomer A; (B) PEG4K (2) in the hydrophobic channel region of monomer B; (C) PEG4K (3) in the hydrophobic channel region connecting the monomers and (D) PEG4K (4) around Lys7 residue from monomer A. The maps were calculated with coefficients $|F_{\text{obs}}| - |F_{\text{calc}}|$ and contoured at 1.0 standard deviations. The ligands molecules were not considered for electron density maps calculation but are drawn for clarity. Drawn using PyMOL program (DeLano, 2002).

monomers and (iii) one PEG4K (PEG 4) molecule interacts with Lys7, Trp77 and several other residues of monomer A (Fig. 3).

Dynamic light scattering experiments indicates a mean hydrodynamic radius (R_H) of 2.3 nm with a polydispersity of 12.0%. This R_H value corresponds to a molecular weight of approximately 23 kDa and is, thus, equivalent to a dimer. These results are in agreement with other literature data for Lys49-PLA₂s since electrophoresis, spectroscopic (Arni et al., 1999; da Silva Giotto et al., 1998), crystallographic (Arni and Ward, 1996; dos Santos et al., 2009; Magro et al., 2003; Murakami et al., 2005), small angle X-ray scattering (Murakami et al., 2007) and dynamic light scattering (Fernandes et al., 2010) experiments demonstrates that bothrops Lys49-PLA₂s are dimeric in solution.

In addition, the inspection of unit-cell packing showed that there are two possible dimeric configurations for the MjTX-II structure. The first possibility is similar to the so-called “conventional dimer” and the second one is similar to the “alternative dimer” (Murakami et al., 2005). In the conventional dimer, the monomers are stabilized by interactions between the tips of β -wings and the residues of the N-terminal helices (Arni and Ward, 1996) while in the alternative dimer they are stabilized by contacts between the putative calcium-binding loops and C-termini forming a connection route between the “active sites” of both monomers (dos Santos et al., 2009). Examination of the unit-cell packing using PISA software (Krissinel and Henrick, 2007) points the alternative dimeric configuration is the most probable to occur in solution. According to this analysis, MjTX-II/PEG4K crystallographic structure presents an interfacial area of 552.6 Å², $G_{\text{int}} = -9.8$ kcal/mol and $G_{\text{diss}} = 0.145$ kcal/mol. Furthermore, this choice is also

supported by previous small angle X-ray scattering experiments (Murakami et al., 2007) and functional aspects of Lys-PLA₂s myotoxins (dos Santos et al., 2009; Murakami et al., 2005).

3.2. Comparison between MjTX-II and MjTX-II complexed to stearic acid structures

The crystal structure of MjTX-II co-crystallized with stearic acid (a fatty acid) has been previously solved (Watanabe et al., 2005) and evidenced six stearic acid molecules interacting with the protein: two of them in each hydrophobic channel (two molecules in each protomer) and other two in the dimeric interface interacting with Lys7 residue. Contrasting with the co-crystallized structure (MjTX-II/stearic acid), the native MjTX-II (this study) only presents four PEG4K molecules: three of them are inside the hydrophobic channels and the fourth one interacts with Lys7 residue (Fig. 1A). However, the comparison of both structures reveals that all ligands occupy similar positions: (i) PEG 1 and PEG 2 occupy the same sites that two stearic acids from the MjTX-II/stearic acid complex (inside of the hydrophobic channels) (Fig. 1B); (ii) PEG 3 is at the hydrophobic channels entrance (N-terminal face of the dimeric structure), connecting both protomers of the dimeric structure and is located approximately at the same position that two stearic acids molecules in the MjTX-II complexed structure (Fig. 1B); (iii) PEG 4 occupies approximately the same position of two stearic acids in the dimeric interface of MjTX-II/stearic acid structure which presents 50% occupancy values and are sited in a tail-to-tail conformation (Fig. 1B) (Watanabe et al., 2005). Due to the alternative dimeric configuration adopted for the native

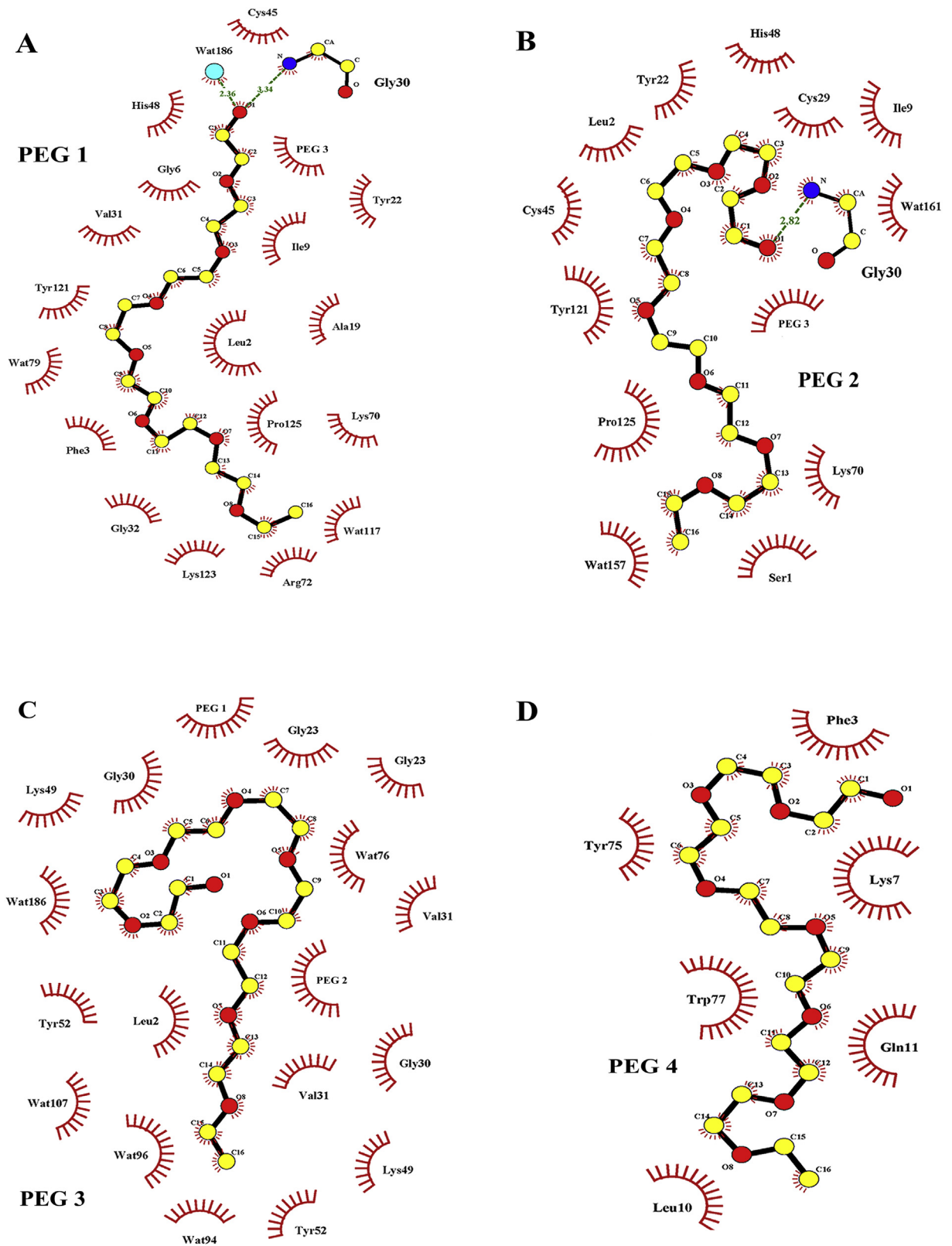


Fig. 3. Interaction of PEG4K molecules in MjTX-II structure. (A) and (B) represents the interactions of PEG4K (1 and 2) molecules that occupies the hydrophobic channel of the structure. (C) Hydrophobic interactions of PEG4K (3) molecule that connects both monomers. (D) Hydrophobic interactions of PEG4K (4) molecule in the protein surface (around Lys7 from monomer A). Drawn using Ligplot program (Wallace et al., 1995).

MjTX-II only one PEG ligand with 100% occupancy was modeled at this site. Therefore, despite the differences between both ligands (PEG4K and stearic acid), both structures are essentially identical as evidenced by the root-mean-square deviation (r.m.s.d.) of 0.52 Å for their C_{α} atoms superposition. Important regions for this toxin biological functions (e.g. the active site, Ca^{2+} -binding loop, C-termini (dos Santos et al., 2009; Fernandes et al., 2010; Magro et al., 2003)) are conserved indicating that PEG4K may structurally simulate a fatty acid molecule bound to toxin's hydrophobic channels since its backbone is structurally similar to the protein substrate (Watanabe et al., 2005). For this reason, we can state that the MjTX-II structure may represent the protein in its active state (attached to the membrane) (dos Santos et al., 2009).

3.3. Comparison of MjTX-II and other Lys49-PLA₂ structures

Several myotoxic Lys49-PLA₂s in the apo and complexed forms have been solved (Arni et al., 1999; dos Santos et al., 2011a; dos Santos et al., 2009; Fernandes et al., 2010; Lee et al., 2001; Magro et al., 2003; Marchi-Salvador et al., 2009; Murakami et al., 2005, 2007; Watanabe et al., 2005). Table 2 shows a structural comparison between the monomers of MjTX-II and the same analysis for several other apo and complexed Lys49-PLA₂s. As previously observed (dos Santos et al., 2009), all complexed structures present lower r.m.s.d. values compared to their respective apo structures. In other words, there is a clear structural pattern for Lys49-PLA₂s whose apo and complexed states can also be distinguished by the “two angle” model previously suggested (dos Santos et al., 2009). Applying this model to MjTX-II structure, the aperture and torsional angles between its monomers are 55° and 25°, respectively. These values are in agreement to those calculated for MjTX-II/stearic acid structure (52° and 20°) and are also similar to values found for other complexed Lys49-PLA₂s (Table 3) (dos Santos et al., 2009).

In 2001, Lee and colleagues solved the PrTX-II/fatty acid structure and suggested an important role played by Lys122. According to the authors, Lys122 interacts with the

main chain carbonyl of Cys29 causing hyperpolarization of the Cys29/Gly30 peptide bond and, consequently, increases the affinity of the toxin for fatty acids (Lee et al., 2001). This hypothesis suggested that Lys49-PLA₂s are enzymes that are able to hydrolyze phospholipids but fail to release the products of its action. The fatty acid would stay retained in the hydrophobic channel of the toxin consequently inhibiting it, therefore explaining why Lys49-PLA₂s toxins do not display significant catalytic activity. In contrast with this hypothesis, Fernandes and colleagues (Fernandes et al., 2010) performed a very comprehensive study using 16 different dimeric Lys49-PLA₂s and showed that Lys 122 is a very flexible residue that may adopt random configurations even though it usually interacts with different negative charged sites. Despite the highlighted absence of pattern for Lys122 interaction, PrTX-II complexed to fatty acid and MjTX-II complexed to stearic acid structures are two observed exceptions (Lee et al., 2001; Watanabe et al., 2005). The Lys122 side chain interacts with main chain carbonyl of Cys29 in both monomers of these dimeric complexes indicating that the phenomena just occur when fatty acids are present in the hydrophobic channels (Fernandes et al., 2010). Interesting, the results presented here for the MjTX-II can clarify this issue. As discussed in the item 3.2, the structure of MjTX-II presents PEG4K molecules in its hydrophobic channels at the same regions where fatty acids are found in the MjTX-II/stearic acid structure. Therefore, this finding suggests that the Cys29-Lys122 interaction is not exclusive for Lys49-PLA₂s-fatty acid bound structures.

Additionally, comparison between BthTX-I/PEG4K (Fernandes et al., 2010) and MjTX-II/PEG4K (this work) structures reveals important features of MjTX-II in comparison to BthTX-I and other bothropic Lys49-PLA₂s myotoxins. Despite the high sequential and structural similarity between MjTX-II and BthTX-I (they share 95% of identity), and the presence of two PEG4K molecules in the hydrophobic channels of both structures, their superposition clearly demonstrates the ligand way of binding at these proteins are somewhat different (Fig. 1C). The reason seems to be the insertion of the residue Asn120 and the Leu32Gly mutation since these characteristics apparently shifts the orientation of PEG molecules inside the hydrophobic channel by modification of the channel ends. Interestingly, Asn120 insertion and Leu32Gly mutation are only found in MjTX-II when comparing this protein to all the other bothropic Lys49-PLA₂s whose structures are solved to date (Fig. 4). Therefore, the Asn120 insertion is probably the responsible for the binding of the interchain PEG 3 molecule since this insertion leads to a distortion of the protein protomers (Table 3). This evidence is enhanced by the fact that other Lys49-PLA₂s toxins that presents 121 amino acids do not bind this interchain PEG4K or PEG3350 (Fernandes et al., 2010) whereas MjTX-II (122 residues) allow a PEG4K interaction at this region. It is important to highlight that bothropic Lys49-PLA₂s that do not have structures solved yet but present mutations and/or insertions at the positions 32 and 120 are known (Fig. 4); however their structural characteristics upon ligand binding will just be evidenced when these structures are elucidated.

Table 2

Superposition between Lys49-PLA₂s monomers (root mean square deviation of C_{α} atoms).

Protein (PDB id)	r.m.s.d. (Å)
MjTX-II/PEG4000	0.23
MjTX-II/Stearic acid (1XXS)	0.26
BaspTX-II/Suramin (1Y4L)	0.68
BthTX-I/ α -tocopherol (3CXI)	0.76
PrTX-I/ α -tocopherol (3CYL)	0.82
BthTX-I/BPB (3HZW)	0.67
PrTX-I/BPB (2OK9)	0.47
BthTX-I/PEG4000 (3IQ3)	0.79
PrTX-I/Rosmarinic acid (3QNL)	0.32
BnIV/Myristic acid (3MLM)	0.55
PrTX-II/Fatty acid (1QLL)	0.25
BaspTX-II (1CLP)	0.60
BnSP-6 (1PC9)	0.96
BnSP-7 (1PA0)	0.96
PrTX-I (2Q2J)	1.04
BthTX-I (3HZD)	1.05

Table 3Torsional angles (θ_T), aperture angles (θ_A) and hydrogen bonds at the interface of Lys49-PLA₂s from *Bothrops* genus.

Protein (PDB id)	θ_T (torsional angle) ^a	θ_A (aperture angle) ^a	Hydrogen bonds at the interfaces ^b		
			Monomer A	Monomer B	Distance Å
MjTX-II	55°	25°	Ala19 [N]	Tyr121 [OH]	2.88
MjTX-II/Stearic acid (1XXS)	52°	20°	Asn17 [ND2]	Tyr121 [OH]	2.29
			Tyr121 [OH]	Asn17 [ND2]	2.36
			Tyr121 [OH]	Ala19 [N]	2.58
			Ala19 [N]	Tyr 121 [OH]	3.64
BaspTX-II/Suramin (1Y4L)	51°	15°	–	–	–
BthTX-I/ α -tocopherol (3CX1)	40°	11°	Tyr119 [O]	Asn17 [ND2]	2.84
			Tyr 119 [OH]	Tyr119 [OH]	2.57
PrTX-I/ α -tocopherol (3CYL)	41°	12°	Tyr119 [O]	Asn17 [ND2]	2.84
			Tyr119 [OH]	Tyr119 [OH]	2.48
BthTX-I/BPB (3HZW)	53°	22°	Tyr119 [OH]	Asn17 [ND2]	3.25
			Tyr119 [OH]	Tyr119 [OH]	3.09
PrTX-I/BPB (2OK9)	41°	29°	Tyr119 [O]	Asn17 [ND2]	2.82
			Tyr119 [OH]	Tyr119 [OH]	2.16
BthTX-I/PEG4000 (3IQ3)	41°	29°	Tyr119 [O]	Asn17 [ND2]	2.82
			Tyr119 [OH]	Tyr119 [OH]	2.56
PrTX-I/Rosmarinic acid (3QNL)	43°	23°	Tyr119 [O]	Asn17 [ND2]	3.16
			Tyr119 [OH]	Tyr119 [OH]	2.18
BnlV/Myristic acid (3MLM)	41°	27°	Asn17 [ND2]	Tyr119 [O]	3.22
			Tyr119 [OH]	Tyr119 [OH]	2.42
PrTX-II/fatty acid (1QLL) ^c	81°	23°	Tyr119 [O]	Asn17 [ND2]	2.49
			Tyr119 [OH]	Tyr119 [OH]	3.09
BaspTX-II (1CLP) ^d	44°	22°	Tyr119 [OH]	Tyr119 [OH]	2.35
			Tyr119 [OH]	Lys20 [NZ]	3.86
BnSP-6 (1PC9)	60°	6°	Tyr119 [O]	Asn17 [ND2]	2.51
BnSP-7 (1PA0)	60°	6°	Lys69 [NZ]	Val31 [O]	2.74
			Tyr119 [O]	Asn17 [ND2]	2.68
PrTX-I (2Q2J)	60°	7°	Val31 [O]	Lys69 [NZ]	2.57
			Asn17 [ND2]	Tyr 119 [O]	2.91
BthTX-I (3HZD)	60°	14°	Asn17 [ND2]	His120 [O]	3.36
			Val31 [O]	Lys69 [NZ]	2.72

^a Torsional and aperture angles were calculated according to the proposal of dos Santos et al., 2009.^b Hydrogen bonds were inferred using the online interactive tool PISA (http://www.ebi.ac.uk/msd-srv/prot_int/cgi-bin/piserver).^c PrTX-II/fatty acid (PDB id 1QLL) crystallographic structure do not follow the torsional/aperture angle pattern for complexed structures as pointed by dos Santos et al., 2009.^d BaspTX-II (PDB id 1CLP) crystallographic structure was deposited as an apo structure but according to dos Santos et al., 2009 it can be a complex.

The C-termini of Lys49-PLA₂s toxins has been pointed as containing their myotoxic site (Arni and Ward, 1996; Magro et al., 2003; Ward et al., 2002). Afterward, dos Santos and colleagues reviewed several native and complexed Lys49-PLA₂s and proposed that Arg118, Lys20 and Lys115 residues constitute these toxins myotoxic site (dos Santos et al., 2009). In the same study, the authors propose a two-step mechanism for Lys49-PLA₂s which allow the destabilization of biological membranes. The first step of the mechanism would be the interaction of the Lys20, Lys115 and Arg118 of these proteins with the phospholipid head group region (dos Santos et al., 2009); subsequently, a quaternary rearrangement takes place in Lys49-PLA₂s monomers allowing long-chain hydrophobic portions of membrane phospholipids to be inserted into the hydrophobic channel of the toxin (dos Santos et al., 2009; dos Santos et al., 2011a). Therefore, the hydrophobic channel was demonstrated to be involved in one of the steps required for Lys49-PLA₂s action mechanism (dos Santos et al., 2009; dos Santos et al., 2011a). It is also interesting to highlight that if the alternative dimer is considered as biological dimer, the myotoxic sites from both monomers are aligned at the same plane (side by side) for the complexed structures (active state) and an interchain Tyr119–Tyr119 hydrogen bond is formed (Table 3) which increasing the toxin potency (dos Santos et al., 2009). The

sequence alignment of bothropic Lys49-PLA₂s (Fig. 4) shows that the residues of the myotoxic site (Lys20, Lys115 and Arg118) and Tyr119 are conserved in MjTX-II, however, the interchain Tyr119–Tyr119 hydrogen bond is not present in its dimeric interface (these residues are at a distance of 4.7 Å). Analyzing MjTX-II sequence (Fig. 4) it is possible to observe that the C-terminal region of this toxin presents some particularities as an insertion of a residue at position 120 and a mutation at position 121 (His→Tyr) if compared to other bothropic Lys49-PLA₂s whose structures are known. Therefore, Asn120 insertion may be the responsible for a diversion of this region as evidenced by the lack of Tyr119–Tyr119 hydrogen bond which is probably compensated by the creation of two new hydrogen bonds with the participation of Tyr121 residue (Table 3).

Then, taking into account these facts (Asn120 insertion and mutations of residues 32 and 121) and their consequences to PEG4Ks mode of binding, it is reasonable to suggest that MjTX-II may require specific or modified inhibitors when compared to molecules that are able to inhibit bothropic Lys49-PLA₂s by interaction with their hydrophobic channels. This is due to the different profile of ligand binding presented at this region (Fig. 1C.) and may have implications when considering structure-based ligand design for Lys49-PLA₂s.

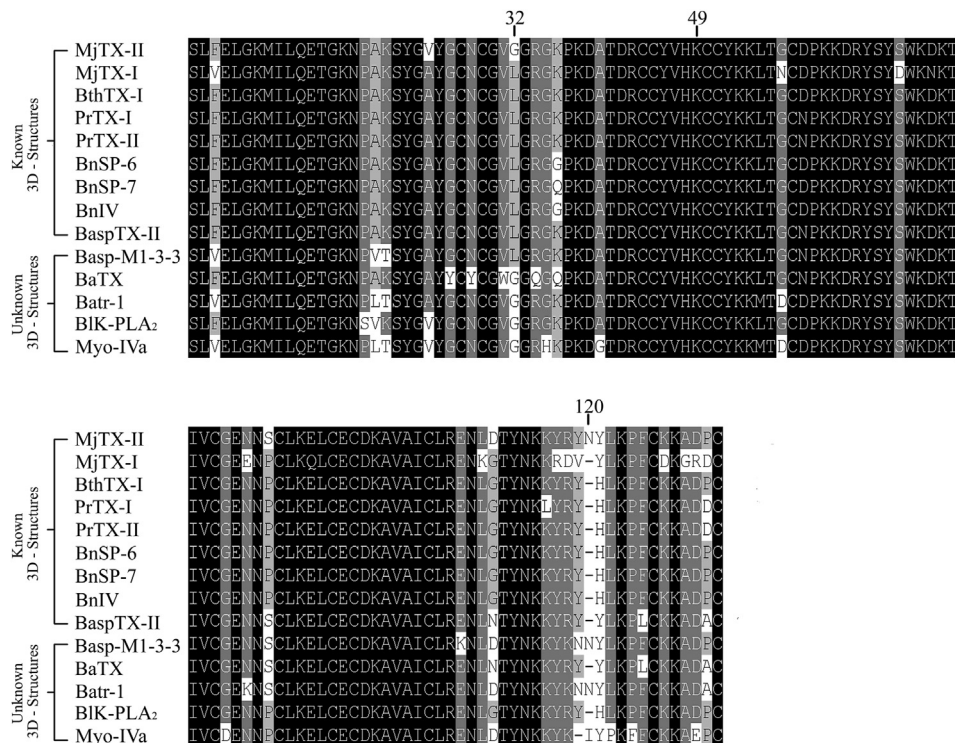


Fig. 4. Amino acid sequence alignment of Lys49-PLA₂s from *Bothrops* genus. The natural substitution Gly32 and the Asn120 insertion are highlighted. NCBI GI entry codes for the proteins represented are BnIV (*Bothrops pauloensis*): 333361256, BnSP-6 (*Bothrops pauloensis*): 49258448, BnSP-7 (*Bothrops pauloensis*): 239938675, BthTX-I (*Bothrops jararacussu*): 51890398, MjTX-II (*Bothrops moojeni*): 62738542; BaspTX-II (*Bothrops asper*): 166215047, PrTX-I (*Bothrops pirajai*): 17433154, PrTX-II (*Bothrops pirajai*): 17368328, Basp-M1-3-3 (*Bothrops asper*): 17433168, BaTX (*Bothrops alternatus*): 292630846, Batr-1 (*Bothrops atrox*): 82201805, BIK-PLA₂ (*Bothrops leucurus*): 353678055, Myo-IVa (*Bothrops asper*): 166216293.

3.4. The crystal structure of MjTX-II and the biological dimer of Lys49-PLA₂ structures

As discussed in the last two sections, MjTX-II structure was solved in the oligomeric assembly known as “alternative dimer” given that it has higher probability of occurrence in solution due to bioinformatic analyses and also due to several experimental and functional reasons (dos Santos et al., 2011a; dos Santos et al., 2009; Fernandes et al., 2010; Marchi-Salvador et al., 2009; Murakami et al., 2005, 2007). However, as discussed in a recent review in this field (Lomonte and Rangel, 2012), this subject is still controversial for some authors.

Although no experiment was able to definitively prove the correct assembly adopted by Lys49-PLA₂s toxins, MjTX-II structure added an important experimental evidence for the choice of the alternative dimer as the probable quaternary assembly found in solution for these proteins. As shown in the Fig. 2, the PEG 3 binds simultaneously to both monomers of the protein. This mode of binding is only possible for the alternative dimeric conformation because if the conventional dimer had been used to solve this structure a large portion of the ligand would be exposed to the solvent which is energetically unfavorable. Similar results were also obtained for PrTX-I/ α -tocopherol and BaspTX-II/suramin structures (dos Santos et al., 2009; Murakami et al., 2005), leading these authors to choose the alternative assembly when solving both complexed structures.

3.5. Functional studies

Myographic studies show that MjTX-II (1.0 μ M) produced an irreversible and time-dependent blockade of both directly ($t_{1/2} = 40.0 \pm 2.3$ min, $n = 7$) and indirectly ($t_{1/2} = 32.1 \pm 4.8$ min, $n = 5$) evoked twitches (Fig. 5A and B). The present findings were consistent with those already described for other Lys49-PLA₂s (Cavalcante et al., 2007; Gallacci et al., 2006; Randazzo-Moura et al., 2008; Rodrigues-Simioni et al., 1995; Soares et al., 2000, 2001; Stabeli et al., 2006). Statistical comparison of the indirectly evoked contractions $t_{1/2}$ of the MjTX-II with those of other Lys49 PLA₂s, such as PrTX-I from *Bothrops pirajai* ($t_{1/2} = 49.0 \pm 6.9$ min, $n = 8$) and BthTX-I from *Bothrops jararacussu* ($t_{1/2} = 40.3 \pm 3.5$ min, $n = 6$), obtained at same experimental conditions, indicates that these toxins have similar potency (Cavalcante et al., 2007). In contrast, MjTX-II presents a more potent neuromuscular blockade when compared to MjTX-I from *B. moojeni*, since at 1.0 μ M this toxin depressed in only about 20% the twitches amplitude after 90 min of contact with the preparation (Salvador et al., 2013). Then, these results indicate MjTX-II has similar or superior neuromuscular blockade action compared to other Lys49-PLA₂s.

It has been suggested that *in vitro* neuromuscular blockade effect observed for Lys49-PLA₂s may be a consequence of their membrane depolarizing activity (Gallacci and Cavalcante, 2010). In order to clarify this issue, we

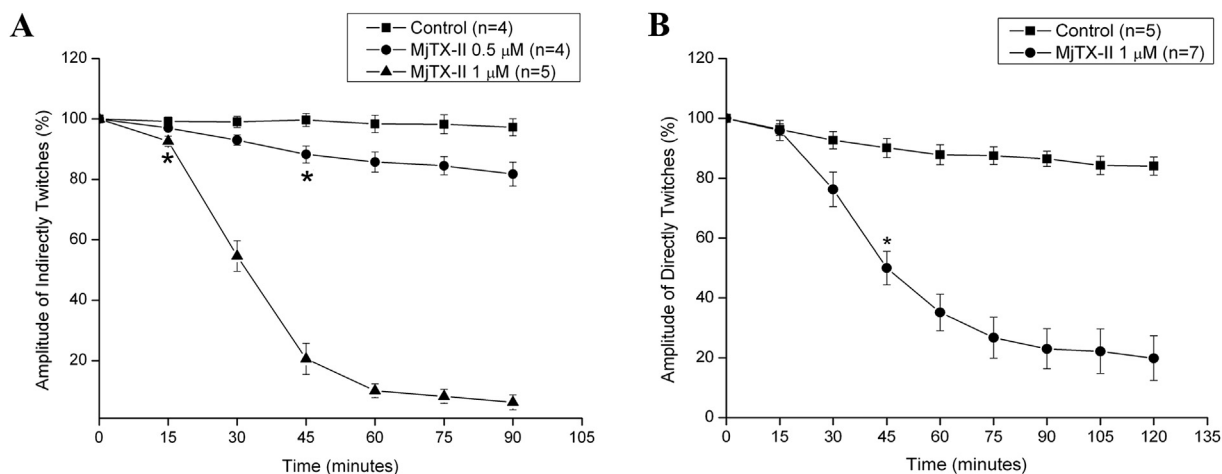


Fig. 5. Effect of MjTX-II on indirectly (A) and directly (B) evoked twitches in mice phrenic-diaphragm preparations. The ordinate represents the % amplitude of twitches relative to the initial amplitude. The abscissa indicates the time (min) after the addition of MjTX-II to the organ bath. Vertical bars represent the SEM, *indicates the point from which there are significant differences relative to control ($P < 0.05$).

performed an electrophysiological study to evaluate membrane depolarizing activity induced by MjTX-II. This technique measures the resting membrane potential of the sarcolemma and has been used as a more direct and sensitive method to assess the initial events in myotoxicity (Aragao et al., 2009). The results show a progressive increase in the resting membrane potential of skeletal muscle fibers from 15 min onwards (Fig. 6) and the increase of the frequency of miniature endplate potentials after 5 min (data not shown), probably as a consequence of the cell depolarization. Taken together, these results show a direct effect of MjTX-II increasing the permeability of the skeletal muscle fibers plasma membrane.

Although the Lys49-PLA₂ mechanism of action is not yet fully elucidated, several studies point the sarcolemma

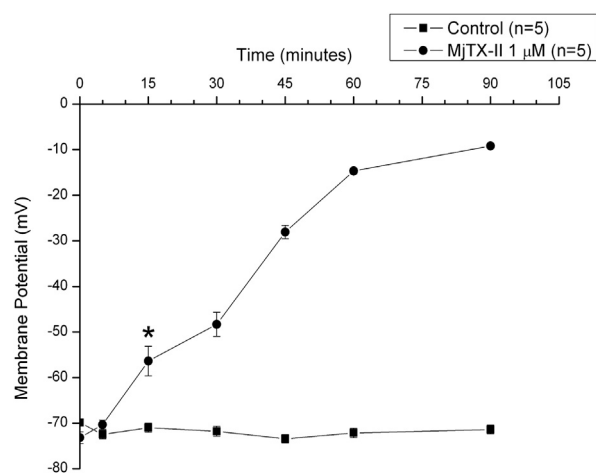


Fig. 6. The resting membrane potential of mice diaphragm muscle preparations under MjTX-II action. The ordinate represents the resting membrane potential (mV) and the abscissa indicates the time (min) after the addition of MjTX-II to the organ bath. The data were grouped as mean \pm SEM ($P < 0.05$). *indicates the point from which there are significant differences relative to control ($P < 0.05$).

as the initial target of these myotoxins (Gutierrez and Lomonte, 1995; Lomonte et al., 2003; Lomonte and Rangel, 2012). A recent study suggests Arg118, together with Lys20 and Lys115, are the residues responsible for protein-membrane anchorage initial steps (dos Santos et al., 2009; dos Santos et al., 2011a). After the establishment of these electrostatic interactions, the protein undergoes a quaternary rearrangement that allows hydrophobic portions of membrane phospholipids to be inserted in the protein hydrophobic channels, therefore culminating with membrane destabilization (dos Santos et al., 2011a). The first consequence of this destabilization is the loss of ionic permeability regulation, leading to a reduction of the resting membrane potential, inactivation of sodium channels and blockade of both directly and indirectly evoked contractions (Gallacci and Cavalcante, 2010). In addition, the disruption of the muscle fiber membranes induced by Lys49-PLA₂ also promotes an increase of cytosolic calcium concentration, initiating a complex series of degenerative mechanisms that culminates with the muscle cell damage (Gutierrez and Ownby, 2003; Lomonte and Rangel, 2012; Montecucco et al., 2008).

4. Conclusions

In this article, we fully characterize functionally and structurally the Lys49-PLA₂ MjTX-II from *B. moojeni*. Despite the fact that this class of proteins has been extensively studied, several issues regarding the function-structure relationships are still need to be clarified, as highlighted by a recent review in this field (Lomonte and Rangel, 2012). This requirement is probably due to the high evolutionary pressure process by which snake venom molecules are submitted, since proteins with few natural amino acid mutations may present different oligomeric configurations, variable toxic potency or even different functions when compared to their ancestral toxins (Doley and Kini, 2009; dos Santos et al., 2011b; Kini, 1997, 2003). An interesting example is the MjTX-I, other myotoxic Lys49-PLA₂ from *B.*

moojeni that presents unusual oligomeric characteristics and displays lower myotoxic activity when compared to all other bothropic Lys49-PLA₂s that have already been structurally and functionally characterized (Andriao-Escarso et al., 2000; Salvador et al., 2013).

As demonstrated in this work, MjTX-II also presents some particularities if compared to other Lys49-PLA₂s which seem to influence the mode of ligand binding along the toxin hydrophobic channel, a feature that may directly affect the design of structure-based ligands for Lys49-PLA₂s.

Acknowledgments

This work was supported by Fundação de Amparo à Pesquisa do Estado de São Paulo (FAPESP), Conselho Nacional de Desenvolvimento Científico e Tecnológico (CNPq), Financiadora de Estudos e Projetos (FINEP), Coordenação de Aperfeiçoamento de Nível Superior (CAPES) – Projeto NanoBiotec, Rede de Biodiversidade e Biotecnologia da Amazônia Legal (BIONORTE/CNPq/MCT), Instituto Nacional para Pesquisa Translacional em Saúde e Ambiente na Região Amazônica (INCT-INPeTAM/CNPq/MCT) e Instituto Nacional para Pesquisa em Toxinas (INCT-Tox), Secretary of Development of Rondonia State (SEPLAN/PRONEX/CNPq).

Conflict of interest

The authors have no conflicts of interest with this work.

References

- Andriao-Escarso, S.H., Soares, A.M., Rodrigues, V.M., Angulo, Y., Diaz, C., Lomonte, B., Gutierrez, J.M., Giglio, J.R., 2000. Myotoxic phospholipases A₂ in *bothrops* snake venoms: effect of chemical modifications on the enzymatic and pharmacological properties of bothrotoxins from *Bothrops jararacussu*. *Biochimie* 82, 755–763.
- Aragao, E.A., Randazzo-Moura, P., Rostelato-Ferreira, S., Rodrigues-Simioni, L., Ward, R.J., 2009. Shared structural determinants for the calcium-independent liposome membrane permeabilization and sarcolemma depolarization in Bothrotoxin-I, a LYS49-PLA₂ from the venom of *Bothrops jararacussu*. *Int. J. Biochem. Cell Biol.* 41, 2588–2593.
- Arni, R.K., Fontes, M.R., Barberato, C., Gutierrez, J.M., Diaz, C., Ward, R.J., 1999. Crystal structure of myotoxin II, a monomeric Lys49-phospholipase A₂ homologue isolated from the venom of *Cerrophidion (Bothrops) godmani*. *Arch. Biochem. Biophys.* 366, 177–182.
- Arni, R.K., Ward, R.J., 1996. Phospholipase A₂—a structural review. *Toxicon* 34, 827–841.
- Arni, R.K., Ward, R.J., Gutierrez, J.M., Tulinsky, A., 1995. Structure of a calcium-independent phospholipase-like myotoxic protein from *Bothrops asper* venom. *Acta Crystallogr. D Biol. Crystallogr.* 51, 311–317.
- Borges, R.C., Araujo, A.F.B., 1998. Seleção de habitat em duas espécies de jararaca (*Bothrops moojeni* Hoge e *B. neuwiedi* Wagler) (Serpentes, Viperidae). *Revista Brasileira de Biologia* 58, 591–601.
- Brunger, A.T., Adams, P.D., Clore, G.M., DeLano, W.L., Gros, P., Grosse-Kunstleve, R.W., Jiang, J.S., Kuszewski, J., Nilges, M., Pannu, N.S., Read, R.J., Rice, L.M., Simonson, T., Warren, G.L., 1998. Crystallography & NMR system: a new software suite for macromolecular structure determination. *Acta Crystallogr. D Biol. Crystallogr.* 54, 905–921.
- Cavalcante, W.L., Campos, T.O., Dal Pai-Silva, M., Pereira, P.S., Oliveira, C.Z., Soares, A.M., Gallacci, M., 2007. Neutralization of snake venom phospholipase A₂ toxins by aqueous extract of *Casearia sylvestris* (Flacourtiaceae) in mouse neuromuscular preparation. *J. Ethnopharmacol.* 112, 490–497.
- Chen, V.B., Arendall 3rd, W.B., Headd, J.J., Keedy, D.A., Immormino, R.M., Kapral, G.J., Murray, L.W., Richardson, J.S., Richardson, D.C., 2010. MolProbity: all-atom structure validation for macromolecular crystallography. *Acta Crystallogr. D Biol. Crystallogr.* 66, 12–21.
- Correia-de-Sa, P., Noronha-Matos, J.B., Timoteo, M.A., Ferreirinha, F., Marques, P., Soares, A.M., Carvalho, C., Cavalcante, W.L., Gallacci, M., 2013. Bothrotoxin-I reduces evoked acetylcholine release from rat motor nerve terminals: radiochemical and real-time video-microscopy studies. *Toxicon* 61C, 16–25.
- da Silva Giotto, M.T., Garratt, R.C., Oliva, G., Mascarenhas, Y.P., Giglio, J.R., Cintra, A.C., de Azevedo Jr., W.F., Arni, R.K., Ward, R.J., 1998. Crystallographic and spectroscopic characterization of a molecular hinge: conformational changes in bothrotoxin I, a dimeric Lys49-phospholipase A₂ homologue. *Proteins* 30, 442–454.
- de Azevedo, W.F., Ward, R.J., Lombardi, F.R., Giglio, J.R., Soares, A.M., Fontes, M.R.M., Arni, R.K., 1997. Crystal Structure of Myotoxin-II: a myotoxic phospholipase A₂-homologue from *Bothrops moojeni* Venom. *Protein Pept. Lett.* 4, 329–334.
- Delano, W.S., 2002. The PyMOL Molecular Graphics System. Delano Scientific, San Carlos.
- Delatorre, P., Rocha, B.A., Santi-Gadelha, T., Gadelha, C.A., Toyama, M.H., Cavada, B.S., 2011. Crystal structure of Bn IV in complex with myristic acid: a Lys49 myotoxic phospholipase A₂ from *Bothrops neuwiedi* venom. *Biochimie* 93, 513–518.
- Doley, R., Kini, R.M., 2009. Protein complexes in snake venom. *Cell Mol. Life Sci.* 66, 2851–2871.
- dos Santos, J.I., Soares, A.M., Fontes, M.R., 2009. Comparative structural studies on Lys49-phospholipases A₂ from *Bothrops* genus reveal their myotoxic site. *J. Struct. Biol.* 167, 106–116.
- dos Santos, J.I., Cardoso, F.F., Soares, A.M., Dal Pai Silva, M., Gallacci, M., Fontes, M.R., 2011a. Structural and functional studies of a bothropic myotoxin complexed to rosmarinic acid: new insights into Lys49-PLA₂ inhibition. *PLoS One* 6, e28521.
- dos Santos, J.I., Cintra-Francischinelli, M., Borges, R.J., Fernandes, C.A., Pizzo, P., Cintra, A.C., Braz, A.S., Soares, A.M., Fontes, M.R., 2011b. Structural, functional, and bioinformatics studies reveal a new snake venom homologue phospholipase A₂ class. *Proteins* 79, 61–78.
- Ducruix, A., Giegé, R., 1992. Crystallization of Nucleic Acids and Proteins: a Practical Approach. Oxford University Press, New York.
- Emsley, P., Cowtan, K., 2004. Coot: model-building tools for molecular graphics. *Acta Crystallogr. D Biol. Crystallogr.* 60, 2126–2132.
- Fatt, P., Katz, B., 1951. An analysis of the end-plate potential recorded with an intracellular electrode. *J. Physiol.* 115, 320–370.
- Fernandes, C.A., Marchi-Salvador, D.P., Salvador, G.M., Silva, M.C., Costa, T.R., Soares, A.M., Fontes, M.R., 2010. Comparison between apo and complexed structures of bothrotoxin-I reveals the role of Lys122 and Ca²⁺-binding loop region for the catalytically inactive Lys49-PLA₂s. *J. Struct. Biol.* 171, 31–43.
- Gallacci, M., Cavalcante, W.L., 2010. Understanding the in vitro neuromuscular activity of snake venom Lys49 phospholipase A₂ homologues. *Toxicon* 55, 1–11.
- Gallacci, M., Oliveira, M., Dal Pai-Silva, M., Cavalcante, W.L., Spencer, P.J., 2006. Paralyzing and myotoxic effects of a recombinant bothrotoxin-I (BthTX-I) on mouse neuromuscular preparations. *Exp. Toxicol. Pathol.* 57, 239–245.
- Gutierrez, J.M., Chaves, F., 1980. Proteolytic, hemorrhagic and myonecrotic effects of the venoms of Costa Rican snakes from the genera *Bothrops*, *Crotalus* and *Lachesis* (author's transl). *Toxicon* 18, 315–321.
- Gutierrez, J.M., Lomonte, B., 1995. Phospholipase A₂ myotoxins from *Bothrops* snake venoms. *Toxicon* 33, 1405–1424.
- Gutierrez, J.M., Ownby, C.L., 2003. Skeletal muscle degeneration induced by venom phospholipases A₂: insights into the mechanisms of local and systemic myotoxicity. *Toxicon* 42, 915–931.
- Gutierrez, J.M., Theakston, R.D., Warrell, D.A., 2006. Confronting the neglected problem of snake bite envenoming: the need for a global partnership. *Plos Med.* 3, e150.
- Harrison, R.A., Hargreaves, A., Wagstaff, S.C., Faragher, B., Lalloo, D.G., 2009. Snake envenoming: a disease of poverty. *PLoS Negl. Trop. Dis.* 3, e569.
- Homs-Brandeburgo, M.I., Queiroz, L.S., Santo-Neto, H., Rodrigues-Simioni, L., Giglio, J.R., 1988. Fractionation of *Bothrops jararacussu* snake venom: partial chemical characterization and biological activity of bothrotoxin. *Toxicon* 26, 615–627.
- Kasturiratne, A., Wickremasinghe, A.R., de Silva, N., Gunawardena, N.K., Pathmeswaran, A., Premaratna, R., Savioli, L., Lalloo, D.G., de Silva, H.J., 2008. The global burden of snakebite: a literature analysis and modelling based on regional estimates of envenoming and deaths. *Plos Med.* 5, 1591–1604.
- Kini, R.M., 1997. Phospholipase A₂ Enzyme: Structure, Function and Mechanism. Wiley, Chichester.
- Kini, R.M., 2003. Excitement ahead: structure, function and mechanism of snake venom phospholipase A₂ enzymes. *Toxicon* 42, 827–840.
- Krissinel, E., Henrick, K., 2007. Inference of macromolecular assemblies from crystalline state. *J. Mol. Biol.* 372, 774–797.
- Lee, W.H., da Silva Giotto, M.T., Marangoni, S., Toyama, M.H., Polikarpov, I., Garratt, R.C., 2001. Structural basis for low catalytic activity in Lys49

- phospholipases A₂-a hypothesis: the crystal structure of piratoxin II complexed to fatty acid. *Biochemistry-US* 40, 28–36.
- Lomonte, B., Angulo, Y., Calderon, L., 2003. An overview of lysine-49 phospholipase A₂ myotoxins from crotalid snake venoms and their structural determinants of myotoxic action. *Toxicon* 42, 885–901.
- Lomonte, B., Gutierrez, J.M., Furtado, M.F., Otero, R., Rosso, J.P., Vargas, O., Carmona, E., Rovira, M.E., 1990. Isolation of basic myotoxins from *Bothrops moojeni* and *Bothrops atrox* snake venoms. *Toxicon* 28, 1137–1146.
- Lomonte, B., Rangel, J., 2012. Snake venom Lys49 myotoxins: from phospholipases A₂ to non-enzymatic membrane disruptors. *Toxicon* 60, 520–530.
- Magro, A.J., Soares, A.M., Giglio, J.R., Fontes, M.R., 2003. Crystal structures of BnSP-7 and BnSP-6, two Lys49-phospholipases A₂: quaternary structure and inhibition mechanism insights. *Biochem. Biophys. Res. Commun.* 311, 713–720.
- Marchi-Salvador, D.P., Fernandes, C.A., Silveira, L.B., Soares, A.M., Fontes, M.R., 2009. Crystal structure of a phospholipase A₂ homolog complexed with *p*-bromophenacyl bromide reveals important structural changes associated with the inhibition of myotoxic activity. *Biochim. Biophys. Acta* 1794, 1583–1590.
- Mebs, D., Ehrenfeld, M., Samejima, Y., 1983. Local necrotizing effect of snake venoms on skin and muscle: relationship to serum creatine kinase. *Toxicon* 21, 393–404.
- Melgarejo, A.R., 2003. Serpentes Peçonhentos no Brasil, Animais Peçonhentos no Brasil: Biologia, Clínica e Terapêutica dos Acidentes. Sarvier, São Paulo, pp. 33–61.
- Montecucco, C., Gutierrez, J.M., Lomonte, B., 2008. Cellular pathology induced by snake venom phospholipase A₂ myotoxins and neurotoxins: common aspects of their mechanisms of action. *Cell Mol. Life Sci.* 65, 2897–2912.
- Murakami, M.T., Arruda, E.Z., Melo, P.A., Martinez, A.B., Calil-Elias, S., Tomaz, M.A., Lomonte, B., Gutierrez, J.M., Arni, R.K., 2005. Inhibition of myotoxic activity of *Bothrops asper* myotoxin II by the anti-trypnosomal drug suramin. *J. Mol. Biol.* 350, 416–426.
- Murakami, M.T., Vicoti, M.M., Abrego, J.R., Lourenzoni, M.R., Cintra, A.C., Arruda, E.Z., Tomaz, M.A., Melo, P.A., Arni, R.K., 2007. Interfacial surface charge and free accessibility to the PLA₂-active site-like region are essential requirements for the activity of Lys49 PLA₂ homologues. *Toxicon* 49, 378–387.
- Otwinowski, Z., Minor, W., 1997. Processing of X-ray diffraction data collected in oscillation mode. *Macromol. Crystallogr. Pt A* 276, 307–326.
- Potterton, L., McNicholas, S., Krissinel, E., Gruber, J., Cowtan, K., Emsley, P., Murshudov, G.N., Cohen, S., Perrakis, A., Noble, M., 2004. Developments in the CCP4 molecular-graphics project. *Acta Crystallogr. D Biol. Crystallogr.* 60, 2288–2294.
- Queiroz, L.S., Petta, C.A., 1984. Histopathological changes caused by venom of urutu snake (*Bothrops alternatus*) in mouse skeletal muscle. *Rev. Inst. Med. Trop. Sao Paulo* 26, 247–253.
- Randazzo-Moura, P., Ponce-Soto, L.A., Rodrigues-Simioni, L., Marangoni, S., 2008. Structural characterization and neuromuscular activity of a new Lys49 phospholipase A₂ homologous (Bp-12) isolated from *Bothrops pauloensis* snake venom. *Protein J.* 27, 355–362.
- Rodrigues-Simioni, L., Prado-Franceschi, J., Cintra, A.C., Giglio, J.R., Jiang, M.S., Fletcher, J.E., 1995. No role for enzymatic activity or dantrolene-sensitive Ca²⁺ stores in the muscular effects of bothropstoxin, a Lys49 phospholipase A₂ myotoxin. *Toxicon* 33, 1479–1489.
- Rosenfeld, G., Kelen, E.M., 1971. Measurement of the coagulation activity of snake venoms: importance to scientific research and therapeutic application. *Rev. Paul. Med.* 77, 149–150.
- Russell, F.E., 1991. Venomous arthropods. *Vet. Hum. Toxicol.* 33, 505–508.
- Salvador, G.H.M., Fernandes, C.A.H., Magro, A.J., Marchi-Salvador, D.P., Cavalcante, W.L.G., Fernandez, R.M., Gallacci, M., Soares, A.M., Oliveira, C.L.P., Fontes, M.R.M., 2013. Structural and phylogenetic studies with MjTX-i reveal a multi-oligomeric toxin – a novel feature in Lys49-PLA₂s protein class. *PLoS One* 8, e60610.
- Saúde, F.N.d., 2001. Manual de Diagnóstico e Tratamento de Acidentes por Animais Peçonhentos. MS/FUNASA, Brasília.
- Soares, A.M., Andriao-Escarso, S.H., Angulo, Y., Lomonte, B., Gutierrez, J.M., Marangoni, S., Toyama, M.H., Arni, R.K., Giglio, J.R., 2000. Structural and functional characterization of myotoxin I, a Lys49 phospholipase A₂ homologue from *Bothrops moojeni* (Caissaca) snake venom. *Arch. Biochem. Biophys.* 373, 7–15.
- Soares, A.M., Andriao-Escarso, S.H., Bortoleto, R.K., Rodrigues-Simioni, L., Arni, R.K., Ward, R.J., Gutierrez, J.M., Giglio, J.R., 2001. Dissociation of enzymatic and pharmacological properties of piratoxins-I and -III, two myotoxic phospholipases A₂ from *Bothrops pirajai* snake venom. *Arch. Biochem. Biophys.* 387, 188–196.
- Stabeli, R.G., Amui, S.F., Sant'Ana, C.D., Pires, M.G., Nomizo, A., Monteiro, M.C., Romão, P.R., Guerra-Sa, R., Vieira, C.A., Giglio, J.R., Fontes, M.R., Soares, A.M., 2006. *Bothrops moojeni* myotoxin-II, a Lys49-phospholipase A₂ homologue: an example of function versatility of snake venom proteins. *Comp. Biochem. Physiol. C Toxicol. Pharmacol.* 142, 371–381.
- Vagin, A., Teplyakov, A., 1997. MOLREP: an automated program for molecular replacement. *J. Appl. Crystallogr.* 30, 1022–1025.
- Wallace, A.C., Laskowski, R.A., Thornton, J.M., 1995. LIGPLOT: a program to generate schematic diagrams of protein-ligand interactions. *Protein Eng.* 8, 127–134.
- Ward, R.J., Chioato, L., de Oliveira, A.H., Ruller, R., Sa, J.M., 2002. Active-site mutagenesis of a Lys49-phospholipase A₂: biological and membrane-disrupting activities in the absence of catalysis. *Biochem. J.* 362, 89–96.
- Watanabe, L., Soares, A.M., Ward, R.J., Fontes, M.R., Arni, R.K., 2005. Structural insights for fatty acid binding in a Lys49-phospholipase A₂: crystal structure of myotoxin II from *Bothrops moojeni* complexed with stearic acid. *Biochimie* 87, 161–167.
- Williams, D., Gutierrez, J.M., Harrison, R., Warrell, D.A., White, J., Winkel, K.D., Gopalakrishnakone, P., 2010. The Global Snake Bite Initiative: an antidote for snake bite. *Lancet* 375, 89–91.